LIGHTWEIGHT STRUCTURES in CIVIL ENGINEERING
CONTEMPORARY PROBLEMS
Monograph from Scientific Seminar
Organized by Polish Chapters of
International Association for Shell and Spatial Structures
University of Warmia and Mazury
Faculty of Geodesy, Geospatial and Civil Engineering
XXII LSCE –2016
Olsztyn, 2 December, 2016

STEEL LATTICE TOWER RELIABILITY ESTIMATION FOR SERVICEABILITY LIMIT STATE

J. Szafran[1] **K. Juszczyk** [2] **M. Kamiński** [3]
[1] Adjunct Professor, [2] M.Sc. Eng, Chair of Structural Reliability, [3] Professor, Head of Chair of Structural Reliability,
Department of Structural Mechanics, Faculty of Civil Engineering, Architecture and Environmental Engineering, Łódź University of Technology

ABSTRACT: The main aim of this study was to estimate structural reliability of a steel lattice telecommunication tower by determining the reliability index β with a SORM approach using full dynamic analysis. A properly calibrated FE computational model created based on tower experimental data, which were obtained from a full-scale test, was used for this purpose. The serviceable limit state of the structure was considered. The main attention was devoted to the displacement of the tower top. A full time analysis was performed during which the structural response was observed against dynamic wind loads which varied in time. A stochastic perturbation method was used to determine statistical parameters: the expected values, the coefficient of variation, the kurtosis, and the skewness over particular moments in time. The key conclusion from the analysis is not only the average wind speeds, but also its distribution in time considerably affected the reliability of a structure.

Keywords: reliability estimation, steel lattice towers, full-scale failure testing, stochastic perturbation method

1. INTRODUCTION

Steel lattice towers are widely used in civil engineering activities like telecommunication (Ref. 14) and the power industry. They are supporting structures for technological equipment such as antennas, cables, wind turbines and etc. most of all. The issues of design of this specific kind of structures are complicated and complex. One of the most important problem from the technological point of view is that the condition about admissible ranges of deflection and rotation was met.

This high, slender, spatial structures are particularly susceptible on wind load, especially on dynamic excitations. Most of towers are usual analyzed by linear static methods, as a constructions which all structural members are subjected to axial forces only and the deformations are slight (Ref. 11). Designing of this type of structures as a simple, slender cantilever beams with one or more concentrated masses is incorrect, as indicated in Ref. 9. Such complex constructions require definitely more precise approach. As lightweight structures, very sensitive to aeroelastic phenomena, they require more deeper analyses to describe their physical behavior.

To obtain more detail information about real behavior of lattice towers, full-scale and laboratory tests are carried out. The example of this type of studies concerning on failure modes of transmission line towers is presented in Ref. 11. The study shows an importance of nonlinear static analysis for understanding the behavior of structure.

Computer models of transmission towers very often are created with reference to experimental data (Refs 1, 4, 7, 8). Tests in full-scale are rather rare, but in scientific literature there are manuscripts with information about design, erection, prefabrication and maintenance of this type of engineering objects. In Ref. 18 the comparison of standards descriptions and definitions were performed with respect to different design codes.

The main type of action affects on lattice tower is the wind load acting on tower body, conductors, antennas, radio units, cable-climbing ladders and etc. Wind actions determine tower geometrical parameters like: cross-section (square, triangular, rectangular), spacing of the supports, degree of legs convergence and above all the type and the size of structural members cross sections. Taking it into account we can assume that the proper determination of the wind actions is extremely important from the reliability point of view. Influence of wind dynamic actions on high, slender, vertical structures may be found in Refs 2, 3, 12 and 13.

Descriptions of dynamic excitations in deterministic sense is rather impossible or possible in very limited scope only, therefore in many cases it is considered as a stochastic. System dynamic excitations usually are described in probabilistic terms by the mean values, the standard deviations of fluctuations and as the correlations in space and time. It can be stated that in analysis of structures subjected to wind dynamic excitations adequate type of the computational, reliability methods and procedures is crucial.

In general sense, the level of structural safety can be measured in terms of reliability which is a metric measure of the probability that a structure fulfils certain performance requirements during its lifetime (Ref. 19). Analyzing the systems with random excitations, determination of the probability of failure (or reliability level) is the key because of the uncertainty of future loads and modeling of the structure.

This paper present the reliability assessment of the steel lattice tower for serviceability limit state that previously was a subject of the full-scale pushover test. Results of that test were used to create the reliability limit state model with the experimentally established data like: displacements of supporting points of the tower, displacements of the top of the tower and initial geometric imperfections.

Maximum displacements of the top of the tower was obtained for the least favorable load direction what is important for further stochastic analysis. Computational considerations were performed for the random wind loading (wind velocity) via full time dynamic analysis (HHT α-method) with FE calibrated model. Main statistics like expected values, variances of displacements for the top of the tower were calculated via perturbation technique. Finally, values of the reliability index were calculated, observed and discussed in full assumed time interval.

2. TOWER STRUCTURE

The analysed object was a lattice, spatial structure of a triangular cross-section (equilateral triangle) and a height of 40.0 m. The body consisted of 7 segments. The first 6 bottom segments (up to 34th m) have constant taper of 5% and form a truncated pyramid of sides of 4.9 m at the base and 1.5 m at the top of the tower. The seventh, top section forms a prism of the base side of 1.5 m. The scheme of the structure is shown in Fig. 1.

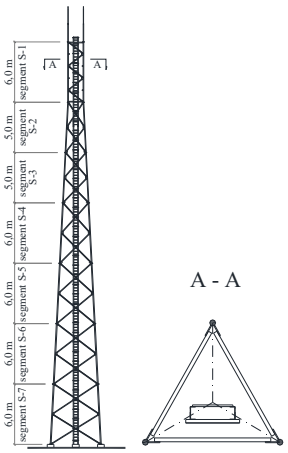

Fig. 1 The analyzed tower scheme.

The legs of the tower were made with round solid bars. The elements of the bracing were made with hot-rolled, equal-panels angle bars and hot-rolled L-bars. The bracing system for the walls in segments S-2 to S-7 is of type X, while the one for the top segment of the tower is of vertical type. The cross braces are continuous in structure and are attached one to another at their points of intersection with a spacer and a bolt. Their attachment to the tower legs was realised using connecting flanges and bolts (two for a joint). The legs at the ends of individual segments were joined using connecting flanges welded at their ends and a suitable number of bolts. The basic elements of the structure are shown in Table 1.

Tab. 1 Particular tower members.

Section	Section height	Cross-sections of legs	Cross-sections of cross braces
S-1 (top)	6.0	Ø65	L60x60x5
S-2	5.0	Ø65	L60x60x5
S-3	5.0	Ø80	L60x60x5
S-4	6.0	Ø80	L90x60x8
S-5	6.0	Ø90	L90x60x8 L100x75x8
S-6	6.0	Ø90	L100x75x8
S-7 (base)	6.0	Ø100	L100x75x8 L120x80x8

3 FULL SCALE TEST

The initial analysis settings were accompanied by measurements taken during a full-scale experiment. It thereafter made it possible to monitor displacements of individual joints of the tower, which otherwise could not be achieved in any way More details about full scale testing may be found in Refs (15, 16, 17). The procedure included simulating external wind impact which constitutes the main load during a normal conditions for this type of structure. It was done using a steel line pulled by a towing truck. Nevertheless, the load type was slightly different than the actual one: the force was applied at one point at a certain angle and exhibited quasistatic characteristics rather than uniformly affecting the whole structure.

The load was imposed on the tower in the least favourable direction so that the maximum displacements of the joints would be achieved (Fig. 2). The line was aligned and placed along "x" direction (Fig. 3) and its position was verified with precise geodetic surveys done in order to avoid accidental, uncontrolled torsion of the tower's body. The load was being increased slowly, in steps, in order to make it possible to control precisely the pressure and the forces in the line. It also allowed for intermediate geodetic measurements of displacements in selected joints of the tower.

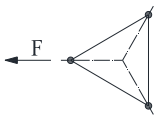

Fig. 2 Direction of load application.

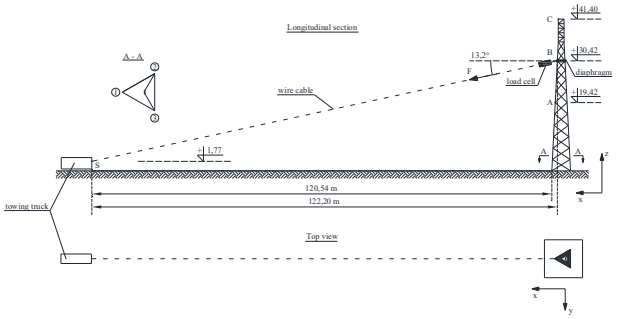

Fig. 3 Scheme of the pushover test.

The displacements of the structure's body were measured at three points located at different heights of the tower on the compressed leg: measurement points A, B, C (Fig. 3). Moreover, the values of their displacements from the initial positions in three directions were registered against the increasing external load (the force in the line). The measurements are presented in Table 2.

Tab. 2 Experimental values of displacements for points A, B, C for the increasing value of the external load.

The force in the line [kN]	The displacements of control points [cm]								
	A			B			C		
	u_x	u_y	u_z	u_x	u_y	u_z	u_x	u_y	u_z
0	0.0	0.0	0.0	0.0	-0.0	0.0	0.0	-0.0	0.0
70	8.6	0.6	-1.1	15.6	-0.4	-0.7	21.6	-0.5	-0.4
80	10.1	0.8	-1.4	18.4	-0.6	-0.8	25.4	-0.4	-0.6
90	12.0	1.0	-1.6	21.6	-0.8	-0.9	29.6	-0.9	-0.8
104	14.4	0.9	-1.5	25.7	-1.1	-1.1	35.4	-1.0	-0.6
110.5	15.8	1.0	-1.8	28.0	-0.8	-0.9	38.4	-1.0	-0.8
116	17.0	0.9	-1.9	30.2	-0.9	-1.1	41.4	-0.8	-0.9
121	18.6	0.6	-1.8	32.8	-0.7	-1.3	44.8	-0.6	-0.9
125	20.0	0.6	-1.9	34.5	-0.6	-1.3	47.4	-0.6	-0.9
132.5	56.7	0.3	-12.6	96.8	-0.9	-10.8	136.5	-0.6	-10.1

4 FINITE ELEMENT MODEL

The model of the structure have been created in program Autodesk Robot Structural Analysis 2015. It was appropriately adjusted to the actual behaviour for the tested type of a tower based on the results obtained during the full-scale resea0rch.

The model consisted of 222 beam, finite elements arranged and connected using 284 nodes. The nodes at the intersections of cross braces were modelled as compatible in order to obtain equal displacement values at these points. Gusset plates, which were used in cross braces installation, were inserted at the middle points of the leg bars. They were attached to the legs with welding. The results of such an attachment method are stresses created during welding process which cause bar strain (denting inwards structure, along bisectors of cross-sections, Fig. 4) constituting initial geometric imperfections of the structure. They were introduced into the computational model at the two bottom segments of the tower where their values, obtained during the measurements of the examined structure, were the highest: 15.0 mm in segment S-7 and 8.0 mm in segment S-6 respectively. The measured strain values were deemed negligible for other segments.

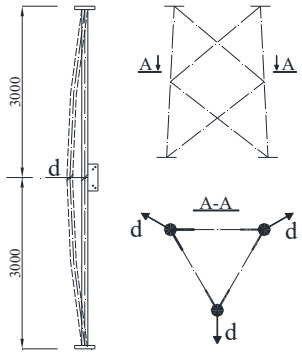

Fig. 4 Initial geometric imperfections at the middle of leg span for section S-7.

Five out of six degrees of freedom were blocked in the modelled structure support: the rotation in three directions (RX, RY, RZ) and movement in horizontal plane (UX, UY). Lastly, the vertical movement was limited by assigning elasticity properties to the support, which allowed for deformation of the ground. They were determined based on the displacements of the support points of the tower against the forces causing the displacements which were observed during the experiment (Table 3). The relation is depicted below:

$$K_{zi} = \frac{F_i}{s_i}, \tag{1}$$

where F_i is the force causing the observed deformations of the ground, and s_i is the value of displacements for supports 1, 2, 3 (Fig. 3).

Tab. 3 The values of the observed displacements of supporting points of the tower for the force in line F_l = 125.0 kN.

The displacements of control points [cm]		
1	2	3
-1.5	1.4	1.1

The structure model was under strong wind loads which were estimated based on the standards in force. The tower equipment configuration, telecommunication devices and supporting structures, which were assumed for the purpose of the analysis, are shown in Fig. 8.

The experiment was simulated in a computational program based on Finite Element Method (Autodesk Robot Structural Analysis 2015) after the adjusted structure model data had been introduced. Two variants of the model were analysed: one with rigid support (model 1) and the other with elastic one (model 2). Apart from the model data, the external load and the forces (for which the displacement measurements were being taken) were also introduced into the program. A static analysis was being carried out when the values of displacements were being observed. Figures 5 - 7 shows the graphs of relationships between the force in the line and displacements for the selected measurements points. They were compared for actual, experimental values and proposed computational models. The range of the external load was from 0.0 to 125.0 kN, because the readout for the force 132.5 kN was made after structure has lost its stability (after plastic deformations had taken place).

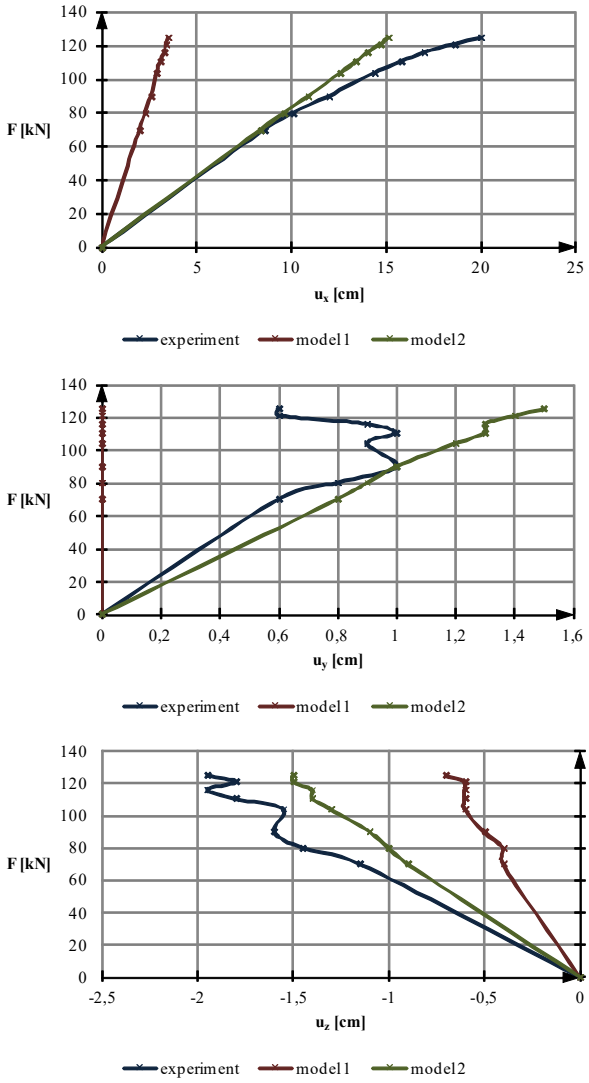

Fig. 5 Displacements for the measurement point A against the external load in directions u_x (top), u_y (centre), and u_z (bottom).

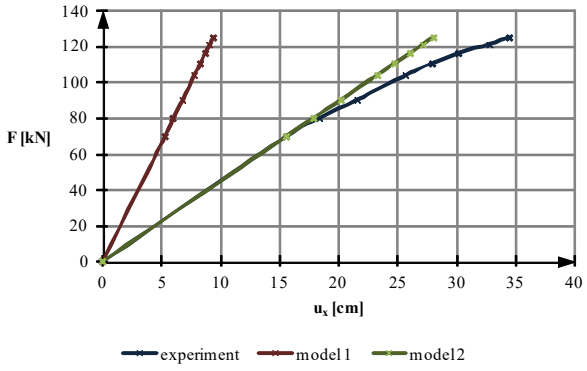

Fig. 6s Displacements for the measurement point B against the external load in direction u_x.

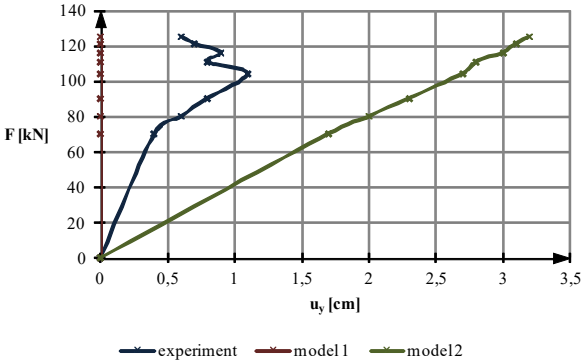

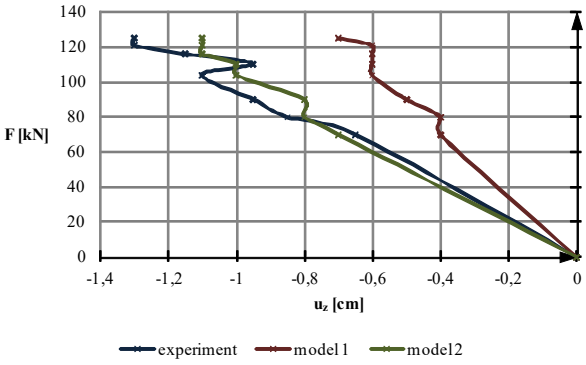

Fig. 6b Displacements for the measurement point B against the external load in direction u_y (top) and u_z (bottom).

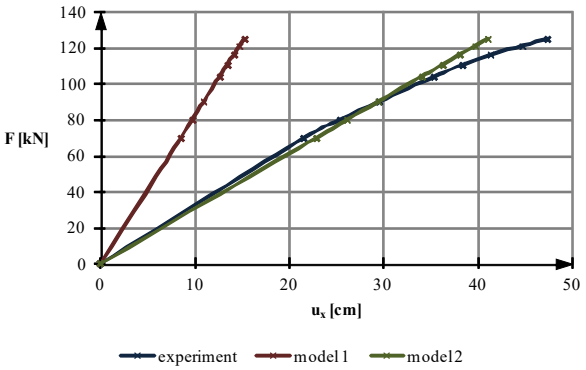

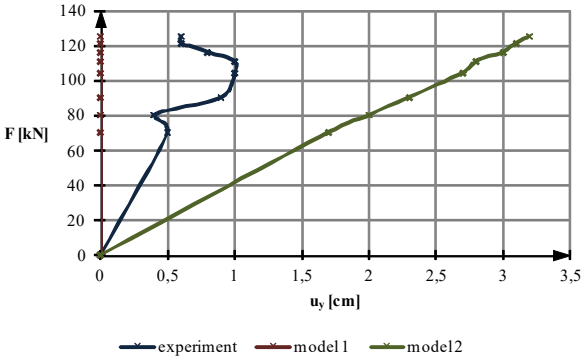

Fig. 7a Displacements for the measurement point C against the external load in directions u_x (top) and u_y (bottom).

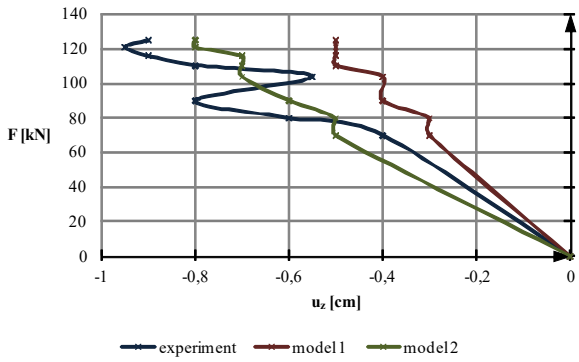

Fig. 7b Displacements for the measurement point C against the external load in directions u_z.

When the above graphs are being analysed, it can be noted that model 2, which has been adjusted to the type of structure based on its full-scale behaviour, provides a considerably better approximation than model 1, which has not been adjusted. It was conclusively essential to take the appropriate elasticity of the tower supports into account. The resulting similarity between the results obtained from model 2 and experimental measurements is particularly visible in the deflection of the tower top in direction x. The differences for direction y were slightly larger. It could have been assumed, however, that these displacements exhibited somewhat random characteristics since even slight deflections from the assumed load application direction (misalignment in line and towing vehicle arrangements) affected them. Taking the above into consideration, it could be concluded that model 2 provided a satisfactory approximate for further computational considerations.

5 DYNAMIC ANALYSIS

While the wind load on the body of the tower was modelled as linear, affecting the legs of the structure, the wind load for the elements of equipment was created as a concentrated force applied to selected nodes (Fig. 9).

Wind load, which is crucial for this type of structures, is not static in action, but rather variable in time. Taking this fact into account, it was decided to carry out a dynamic analysis on the tower which took dynamic nature of the wind into consideration.

Full time analysis has been carried out where the structure responses, in form of horizontal displacements of the top (corresponding to displacements u_x of point C), have been observed against wind load which was changing over time. A function of wind speed variation was defined for the analysed time range of ten minutes (600 seconds). It was based on the speed record probed for a strong wind conditions at a fixed point in space in November (Ref. 10) (Fig. 10).

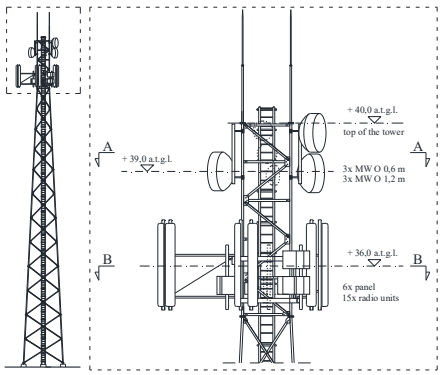

Fig. 8a The configuration of telecommunication devices and supporting structures in the analysis (front view).

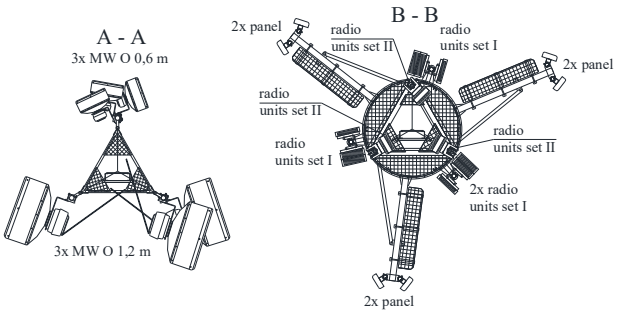

Fig. 8b The configuration of telecommunication devices and supporting structures in the analysis (cross sections).

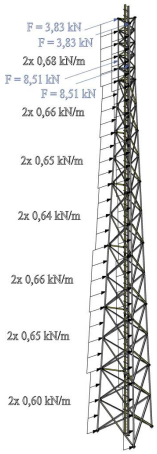

Fig. 9 Draft of the wind load for the computational model of the tower structure.

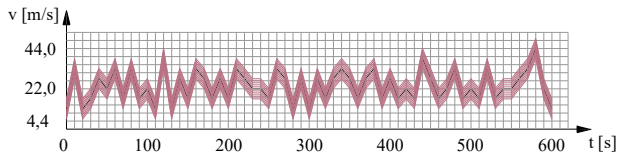

Fig. 10 The assumed function for wind speed variation over time for the analysed time range of ten minutes.

The wind load based on the standards in force has been assessed assuming an average velocity value of v = 22 m/s. A series of analyses have been performed for 11 cases of wind load which had been generated by multiplying the function of variation by the following factors: 0.5; 0.6; 0.7; 0.8; 0.9; 1.1; 1.2; 1.3; 1.4; 1.5. In this way the values of average wind speeds for the individual cases differed correspondingly by 10 % of their base values.

An analysis consisting of a nonlinear integration of motion equations, taking into account effects of third order (P-delta): an additional transverse stiffness and stresses created with deformation, has been carried out. Apart from geometric nonlinearities, constructional nonlinearities in form of nonlinear nodes (supports with a defined stiffness function and compatible nodes) were also present in the model. The following solution to the equation of time variable t has been obtained for each time step equal to 0.1 seconds:

$$M \cdot a(t) + C \cdot v(t) + N(d(t)) = F(t)\,, \tag{2}$$

where the initial values are known: $d(0) = d0$ and $v(0) = v0$; M - mass matrix; d, v, a, F - vectors for correspondingly: displacements, speed, acceleration, and load; $C = \alpha \cdot M + \beta \cdot K$ - damping matrix; K - stiffness matrix; α and β – parameters; N - internal forces vector, which is in a nonlinear relation with displacement vector d.

Integration of motion equations was done using Hilber-Hughes-Taylor method, where the discrete form of the motion equation is:

$$\begin{aligned}&\mathbf{M}\ddot{\mathbf{q}}_{\mathbf{n+1}} + (1+\alpha)\mathbf{C}\dot{\mathbf{q}}_{\mathbf{n+1}} - \alpha\mathbf{C}\dot{\mathbf{q}}_{\mathbf{n}} + (1+\alpha)\mathbf{K}\mathbf{q}_{\mathbf{n+1}} - \alpha\mathbf{K}\mathbf{q}_{\mathbf{n}} \\ &= \mathbf{f}(t_{n+1} + \alpha\Delta t),\end{aligned} \tag{3}$$

where $-1/3 \le \alpha \le 0$. The value of parameter was assumed as α = -0.3 for the purpose of the analysis.

The values for displacements, speed, and acceleration for the next time step were obtained from the following relations:

$$\begin{aligned}\mathbf{q}_{n+1} &= \mathbf{q}_n + h\dot{\mathbf{q}}_n + \frac{h^2}{2}\left[(1-2\beta_{HHT})\ddot{\mathbf{q}}_n + 2\beta_{HHT}\ddot{\mathbf{q}}_{n+1}\right], \\ \dot{\mathbf{q}}_{n+1} &= \dot{\mathbf{q}}_n + h\left[(1-\gamma_{HHT})\ddot{\mathbf{q}}_n + \gamma_{HHT}\ddot{\mathbf{q}}_{n+1}\right].\end{aligned} \tag{4}$$

where:

$$\beta_{HHT} = \frac{(1-\alpha)^2}{4}\,, \tag{5}$$

$$\gamma_{HHT} = \frac{1-2\alpha}{2}\,. \tag{6}$$

This method allows for removing the unfavourable impact of high frequencies thus not affecting the quality of the solution.

6 STATISTICAL PARAMETERS

A generalized stochastic perturbation technique (Refs. 5,6) based on a Taylor expansion and the traditional finite element method was used to obtain statistics of the tower nodes displacements under dynamic loading. Polynomial response functions of the observed design parameters such as deflections of the top of the structure were numerically determined via symbolic algebra system MAPLE with least square method embedded into the system. Statistical parameters such as expected values, coefficients of variation, skewness, and kurtosis for each time points were determined; the assumed time step at which parameters were analyzed was equal to 5 seconds.

A 9th order polynomial was used as an approximation function, and an analysis to 16th order was carried out in order to define the statistical parameters. Figs 11-14 shows the graphs of relationships of particular statistical parameters against time: the expected values, coefficients of variation, skewness, and kurtosis.

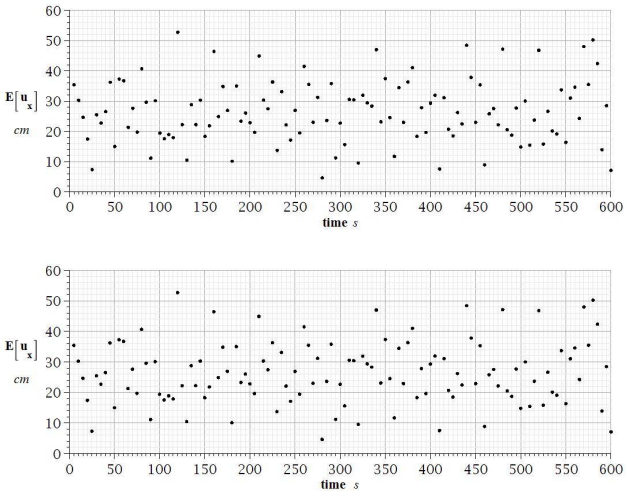

Fig. 11a Relationships between the expected values for horizontal displacements of the top of the tower against the initial values of coefficient of variation equal to α = 0.05, (top) and α = 0.10 (bottom).

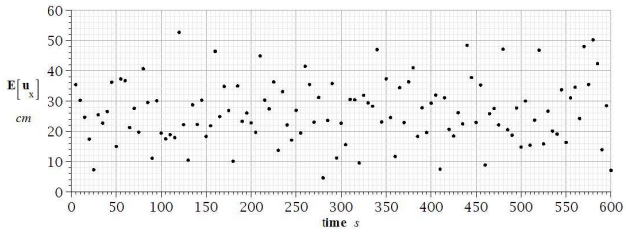

Fig. 11b Relationships between the expected values for horizontal displacements of the top of the tower against the initial values of coefficient of variation equal to α = 0.15.

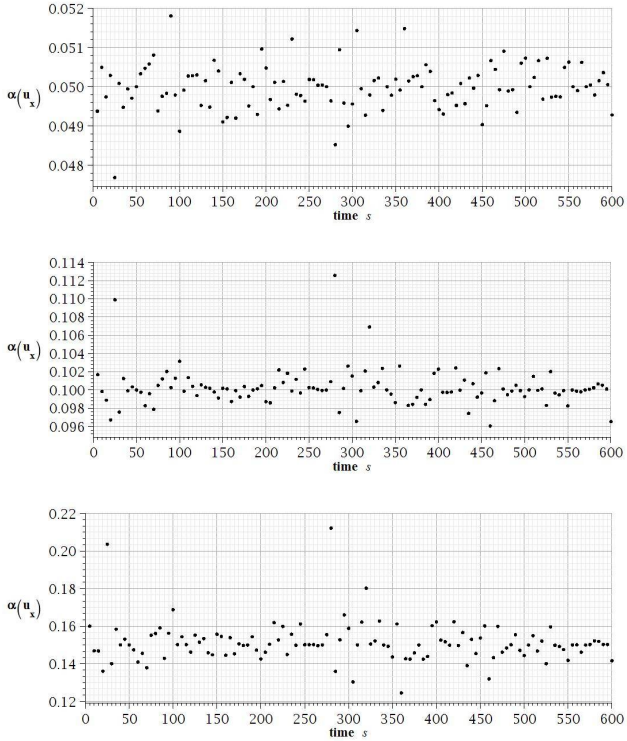

Fig. 12 Coefficients of variation against time for horizontal displacements of the top of the tower and initial values of coefficient of variation equal to α = 0.05 (top), α = 0.10 (centre) and α = 0.15 (bottom).

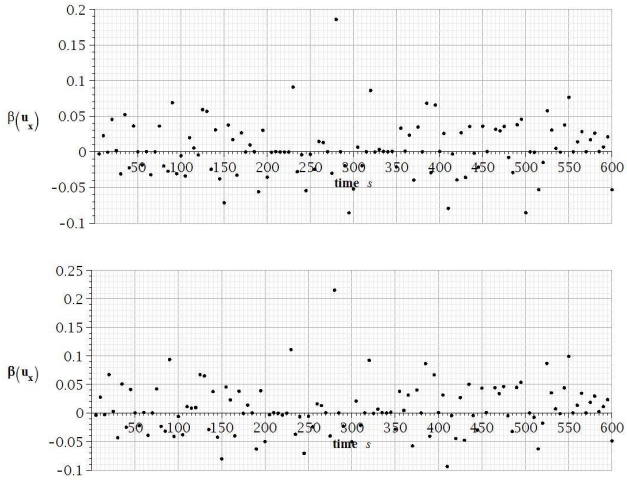

Fig. 13a Skewness against time for horizontal displacements of the top of the tower and initial values of coefficient of variation equal to α = 0.05 (top) and α = 0.10 (bottom).

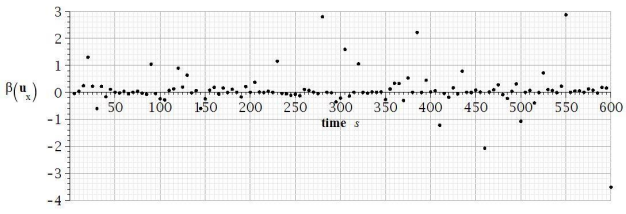

Fig. 13b Skewness against time for horizontal displacements of the top of the tower and initial values of coefficient of variation equal to α α = 0.15.

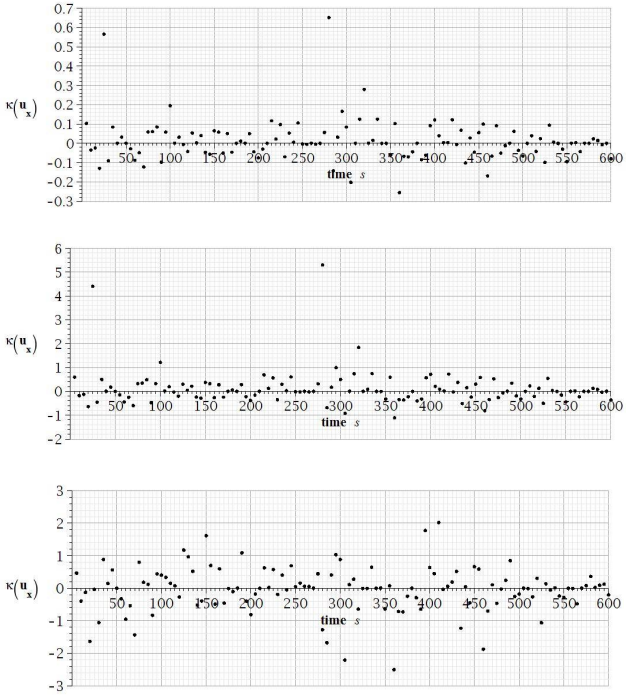

Fig. 14 Kurtosis against time for horizontal displacements of the top of the tower and initial values of coefficient of variation equal to α = 0.05 (top), α = 0.10 (centre), and α = 0.15 (bottom).

Analysing the above graphs we can state that either the expected values are independent of coefficient of variation for this case, or that its influence is insignificant - the graphs are practically identical for parameters α = 0.05, α = 0.10, and α = 0.15 (Fig. 11). Conversely, the differences from the expected displacements values are visible in standard deviation values. One can see, based on the variation coefficient graphs, that the higher the value of input coefficient α, the larger the scatter of output results. However, we can separate individual time points where the value of output coefficient α is visibly higher than others (for higher input coefficients α = 0.10 and α = 0.15), (Fig. 12).

Attention should be also devoted to global wind speed amplitude over the whole time spectrum which was considered. It is quite significant for the assumed variation function and the average base wind speed, and is equal to 44 m/s (Fig. 15). Such a great difference between the minimum and maximum speed results in a significant scatter of the expected values in the analysed time range.

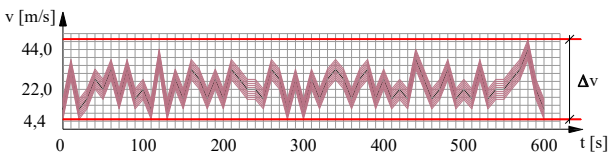

Fig. 15 Time fluctuations of the wind speed.

In case of skewness, the estimated values for input parameters of α equal to α = 0.05 and α = 0.10 are similar and vary by only about -0,1 to 0,2 in the given time range (Fig. 13). In case where the input variation coefficient is equal to α = 0.15 the increase in skewness is significant: from roughly -3,5 to 3 wherein only sparse, single points assume the extreme values. It can be therefore concluded that the skewness of probability distribution of the resulting values of displacements increases with the increase in spread of the input parameters, and the relationship is not linear.

When the kurtosis graphs are analysed, we can notice that their values do not grow proportionally to the scatter of input parameter α as in case of skewness (Fig. 14). The minimal values occur for variation coefficient equal to α = 0,05 (the range from about -0.3 to 0.7) and the values grow considerably for the coefficient equal to α = 0.10 (the range from about -1.0 to 5.0), and subsequently decrease in value again (values from about. -2.5 to 2.0). It is also worth noting that the extreme values can be found only at time points in case of parameters equal to α = 0.05 and α = 0.10, whereas the scatter over the observed time range is more balanced for α = 0.15.

The crucial part of the analysis was to determine reliability indices β_{SORM} by SORM approach for individual time moments. They were defined similarly as the statistical parameters discussed above - for input coefficients of variation equal α = 0.05, α = 0.10, and α = 0.15 (Fig. 16). As the limit, the experimental value of displacements for external load equal to F_1 = 125.0 kN had been assumed and was established as a maximal deflection value at which the requirement for serviceably limit state is fulfilled.

Reliability index was defined as a reciprocal in inverse proportion to the safety margin. For the considered case we can express it in the following manner:

$$\beta_{FORM} = \frac{E[u_{x,\exp}] - E[u_x]}{\sqrt{\sigma[u_{x,\exp}]^2 + \sigma[u_x]^2}}, \qquad (7)$$

where: $E[u_{x,exp}]$ denotes the expected value of the experimental maximal deflection, $E[u_x]$ is the expected value of the horizontal displacement for the top of the tower according to the random wind velocity and $\sigma[u_{x,exp}]$, $\sigma[u_x]$ are the standard deviations of the above variables respectively.
The standard deviation value was assumed as a percentage difference between the deflection registered for the external load equal to 125.0 kN and the predicted deflection in an elastic state for the load equal to the breaking force (132.5 kN) - σ = 0.06.

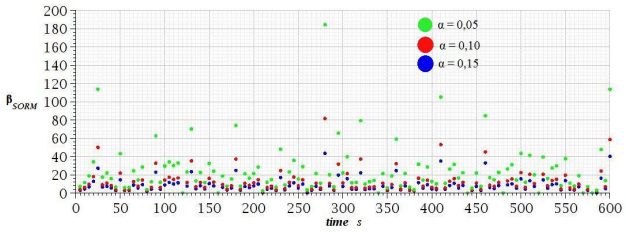

Fig. 15 Relationship of reliability indictor SORM against time, showing the input variation coefficients equal to α = 0.05 (green), α = 0.10 (red), and α = 0.15 (blue).

The graphs of reliability indices determined for higher values of variation coefficient are correspondingly smaller which means that the higher the dispersion of input parameters, the lower the analysed structure reliability at separate time points. It should be added, that the relationship is not linear. Fig. 17 presents the graphs of the reliability indices over time against the values of the expected horizontal displacements for the input parameter α = 0.15 over the analysed time range.

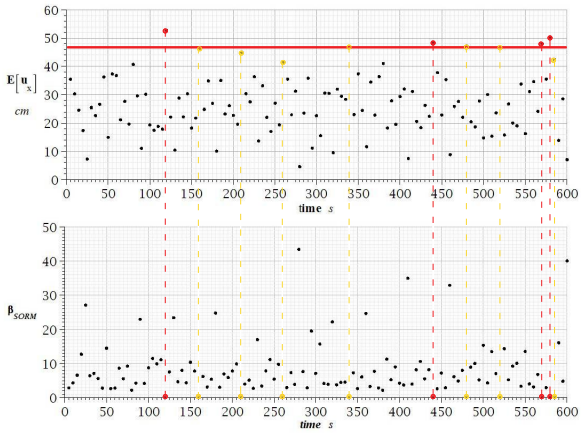

Fig. 17 **E**xpected values of horizontal displacements of the top of the tower against the reliability indices for input parameter α = 0.15.

The maximum horizontal deflection of the tower during the experiment was marked with a horizontal red line. It was registered when the force in the line was 125.0 kN. Out of the 11 time points where the reliability index was 0 (which meant that the structure did not meet the reliability requirements for this scope) only 4 had the expected values of displacements exceed the allowed, boundary value. In the other 7 points the displacements were close or equal to the boundary value.

6 CONCLUSIONS

The displacement observations of a tower used as a supporting structure for telecommunication devices are important from the technological point of view; the admissible ranges of deflection and rotation correspond to the basic requirements that must be met when it comes to determination of the serviceable limit state for an object.

This article was entirely devoted to a reliability analysis of a steel telecommunication tower in a serviceability limit state. The analysis was based on a reliability index which was determined using SORM method. Particular attention was devoted to the way in which random wind velocity and assumed function of dynamic excitation affect reliability index values. The dynamic analysis used took into account the distribution of wind speed values in time which was essential; during the observation of reliability indices in a given time range we could notice that the results yielded measurement points where β_{SORM} was not zero, while the average speed was at least equal to speed values at which the indices are equal to zero for other times. This phenomenon was caused by the fact that the previous time range results affect the ones for the next time range. Therefore not only the average wind speeds, but also its distribution in time considerably affected the reliability of a structure.

The reliability indices were 0 at all points in time where the expected values of the horizontal displacements exceeded the experimental deflection of the top of the tower. There existed, however, moments in time, where the indices were equal to zero. While it provides evidence to the fact that the structure did not fulfil the conditions for reliability, the expected values did not exceed the boundary values for displacements. If we base the observations only on the central moment, we do not take into consideration the possible scatter of boundary displacement values which might have been caused by various construction defects, such as geometrical or material imperfections, or randomness which is unavoidable for this type of loads.

The assumed function of wind speed variation over time essentially affected the results as well, which were characterized by considerable fluctuations and speed amplitudes for this case. Such an assumed characteristic of the wind results in great scatter of global values for the expected displacement. It additionally creates a higher number of time ranges where the reliability index approaches or reaches value 0. Therefore it seems that a selection of wind against time function is decisive for this type of analyses.

REFERENCES

1. F. Albermani, S. Kitipornchai, R.W.K. Chan: Failure analysis of transmission towers. Engineering Failure Analysis, 16, 2009, pp. 1922-1928.
2. M. Belloli, Z. Rosa, A. Zasso: Wind loads on high slender tower: Numerical and experimental comparison. Engineering Structures, 68, 2014, pp. 24-32.
3. J.D. Holmes: Along-wind response of lattice towers – III. Effective load distributions. Engineering Structures 18(7), 1996, pp. 489-494.
4. W.Q. Jiang et al.: Accurate modelling of joint effects in lattice transmission towers. Engineering Structures 33, 2011, pp. 1817-1827.
5. M. Kamiński: The Stochastic Perturbation Method for Computational Mechanics. Wiley, 2013.
6. M. Kamiński, J. Szafran: Random eigenvibrations of elastic structures by the response function method and the generalized stochastic perturbation technique. Archives of Civil and Mechanical Engineering 9, 2009, pp.5-32.
7. S. Kitipornchai, F. Albermani: Nonlinear finite element analysis of latticed transmission towers. Engineering Structures 15, 1993, pp. 259-269.
8. P.S. Lee, G. McClure: Elastoplastic large deformation analysis of a lattice steel tower structure and comparison with full-scale tests. Journal of Constructional Steel Research 63, 2007, pp. 709-717.
9. C.H. Nguyen et al.: Aeroelastic instability and wind-excited response of complex lighting poles and antenna masts. Engineering Structures 85, 2015, pp. 264-276.
10. Ch. Petersen: Entwicklung eines Böfaktors durch Time - History - Schwingungssimulation realer Windgeschwindigkeitschreibe, BAAB, H. 7, München 1975.
11. N. Prasad Rao et al.: Studies on failure of transmission line towers in testing. Engineering Structures 35, 2012, pp. 55-70.
12. M.P. Repetto, G. Solari: Dynamic along wind fatigue of slender and vertical structures. Engineering Structures 23, 2001, pp. 1622-1633.
13. M.P. Repetto, G. Solari: Wind-induced fatigue collapse of real slender structures. Engineering Structures 32, 2010, pp. 3888-98.
14. B.W. Smith: Communication structures. Thomas Telford Publishing, London 2007.
15. J. Szafran, K. Juszczyk, M. Kamiński: Full-scale testing of steel lattice towers: requirements, preparation, execution, challenges, and the results. Lightweight Structures in Civil Engineering - Conterporary Problems - Monograph from Scientific Conference of IASS Polish Chapters, Rzeszów University of Technology, pp. 101-107.
16. J. Szafran, K. Rykaluk: A full-scale experiment of a lattice telecommunication tower under breaking load. Journal of Constructional Steel Research 120, 2016, pp. 160-175.
17. J. Szafran: An experimental investigation into mechanism of a full-scale 40 m high steel telecommunication tower. Engineering Failure Analysis 54, 2015, pp. 131-145.
18. R. Travanca, H. Varum, P.V. Real: The past 20 years of telecommunication structures in Portugal. Eng. Structures 48, 2013, pp. 472-485.
19. M.A. Valdebenito et. al.: Reliability sensitivity estimation of linear systems under stochastic excitation. Computers and Structures 92-93, 2012, pp. 257-268.

[1]) J. Szafran, email: *jacek.szafran@p.lodz.pl,* POLAND
[2]) K. Juszczyk, email: *email: kjuszczyk@compactprojekt.pl,* POLAND
[3]) M. Kamiński, email: *marcin.kaminski@p.lodz.pl,* POLAND

View publication stats